ECLÉTICA QUÍMICA

Eclet. Quim. 49 | e-1529, 2024

Review Article

https://doi.org/10.26850/1678-4618.eq.v49.2024.e1529

Last decade insights on cemented carbides: A review on alternative binders, new consolidation techniques and advanced characterization

Daniela Andreina Sandoval **Ravotti**[1], Hortensia Melero **Correas**[1], Núria Cinca **Luis**[1+]

Abstract

Cemented carbide alloys are well known powder metallurgically processed materials used for a wide range of tooling and components that require a good balance of hardness and fracture toughness, together with wear resistance. After 100 years of the first patent, research and development within this area continues to fulfil more demanding applications and adapt to new requirements. The last decade especially has witnessed important advances. In that sense, Co-free compositions are being studied due to the health issues that its use implies and its criticality in the supply chain. Secondly, the steps towards near-net-shape components by means of additive manufacturing technologies to avoid waste of powder and the technological advance of fast sintering processes are promising. Finally, new microstructural and mechanical characterization methods at micro and nanoscale provide helpful insights for a better understanding of these materials under performance.

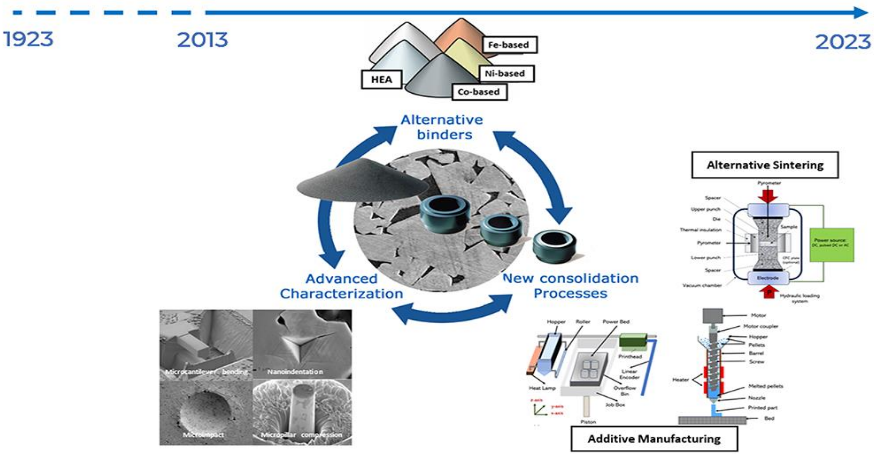

Article History

Received November 03, 2023
Accepted April 25, 2024
Published July 04, 2024

Keywords

1. cemented carbides;
2. alternative binders;
3. consolidation routes;
4. micro mechanical;
5. tribological properties.

Section Editor

Mário Antônio Alves da Cunha

Highlights

- More demanding wear and corrosion resistant applications incentive new developments in tooling industry.
- Novel binders, mainly those based on high entropy alloys, are promising for cobalt substitution.
- New powder metallurgy routes overcome limitations of conventional production methodologies.
- Micro and nano-scale testing characterization increases the understanding of failure mechanisms.

CONTENTS

[1]Hyperion Materials & Technologies, Polígono Industrial Roca, Martorelles, Barcelona, Spain.
+Corresponding author: Núria Cinca Luis, **Phone:** +34935717600, **Email address:** nuria.cinca@hyperionmt.com

1. Introduction

Cemented carbides (also referred to as hardmetals) are a group of composite materials that show outstanding mechanical properties such as hardness and fracture toughness and excellent wear resistance. Such combination of properties makes them suitable to produce component and tool materials capable of working under stringent requirements for high demanding applications.

The microstructure of cemented carbides is heterogeneous. It is constituted by hard, brittle carbides bonded by a soft and tough metallic binder. The first ones are refractory carbides of transition metals (WC, TiC, TaC, Cr_3C_2 or Mo_2C), and the last one is a metal from the iron group, more often cobalt (Co) or nickel (Ni) and their alloys (Exner, 1979).

Refractory carbides of transition metals from the groups IV, V and VI show an interstitial structure that combines metallic, covalent, and ionic bonds, providing them with a high melting point. They also exhibit high hardness and strength with high thermal and chemical stability. The metallic binder phase is a ductile and softer phase that contributes to improve the toughness of cemented carbides (Upadhyaya, 1996).

The unique combination of hardness and toughness given by its constitutive phases (in comparison with other hard materials), positions cemented carbides as the most versatile materials used mainly in the tooling, mining, and oil and gas industries (Hyperion Materials & Technologies, 2019). Figure 1 presents the different application sectors in which cemented carbides are used, according to their Co content and WC grain size, as well as hardness; it can be observed that by tailoring these parameters, cemented carbides can be applied in a broad range of applications.

The development of cemented carbides started during World War I in Germany due to the need to replace diamond drawing dies with a less expensive material in the production of tungsten (W) filaments (Exner, 1979; Ortner *et al.*, 2014). Several attempts were made without success, until 1923, when tungsten carbide (WC) with added Ni was sintered. With time, Ni was replaced by Co, obtaining a good ceramic-metal combination, suitable to produce fine W wires of good quality (Ettmayer *et al.*, 2014; Ortner *et al.*, 2014). The new material was commercialized in 1926 under the name "WIDIA" (from German terminology "wie Diamant" – meaning like diamond).

With the 100th anniversary of its invention (Konyashin, 2023), it became evident that there are many opportunities to improve cemented carbides by tailoring their composition and microstructure through substitution and/or alloying of both carbide and binder phases, as well as by using novel processing and characterization methods. In the following review, we present current industrial knowledge around cemented carbides before focusing on the main developments evidenced during the last decade.

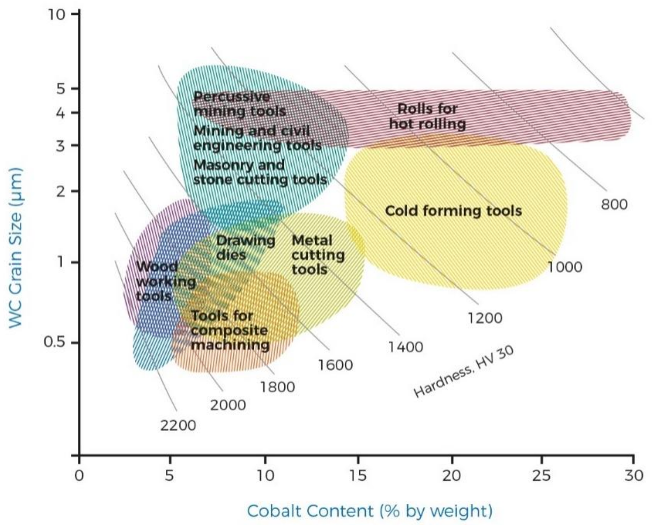

Figure 1. Range of applications in which cemented carbides are used, defined by WC grain size, Cobalt content and hardness. **Source:** Adapted from Sandvik (s.d.) and Hyperion Materials & Technologies (2019).

2. General insights on conventional knowledge of cemented carbides

2.1. Common constituents

In cemented carbides, the most used ceramic phase is tungsten carbide (WC) (Upadhyaya, 2001), while the metallic binder is often cobalt (Co), followed by nickel (Ni) and iron (Fe) in order of importance (Prakash, 2008). These are still the most successful composite materials produced by powder metallurgy technologies.

The binder is selected for its wettability on the carbide and interfacial adhesion characteristics. In this regard, Co shows outstanding wetting of WC, resulting in full densification during conventional liquid phase sintering methods, leading to higher values of toughness when comparing with other metallic binders (García *et al.*, 2019; Lay and Missiaen, 2014). The formation of other undesirable phases, such as graphite or eta phase, occurs when the WC-Co system is exceeding or depleting in carbon content, respectively (García *et al.*, 2019; Lay and Missiaen, 2014).

WC particles exhibit a hexagonal close packed (HCP) crystal structure; WC crystals grown from liquid-metal solutions exhibit the shape shown in Fig. 2a, which is also the shape of WC grains in cemented carbides as seen in Fig. 2b and 2c. The shape adopted by WC in cemented carbides owes to the high polarity of the prismatic crystal planes of (1010) type due to the different spacing of the W and C planes of [1010] directions; therefore, there are two sets of equivalents (1010) planes, instead of six ones. Because of its non-centrosymmetric structure of WC, the microhardness is strongly anisotropic, i.e., the hardness of the basal plane (0001), the prismatic plane (1010) and intermediate orientations are different (Exner, 1979).

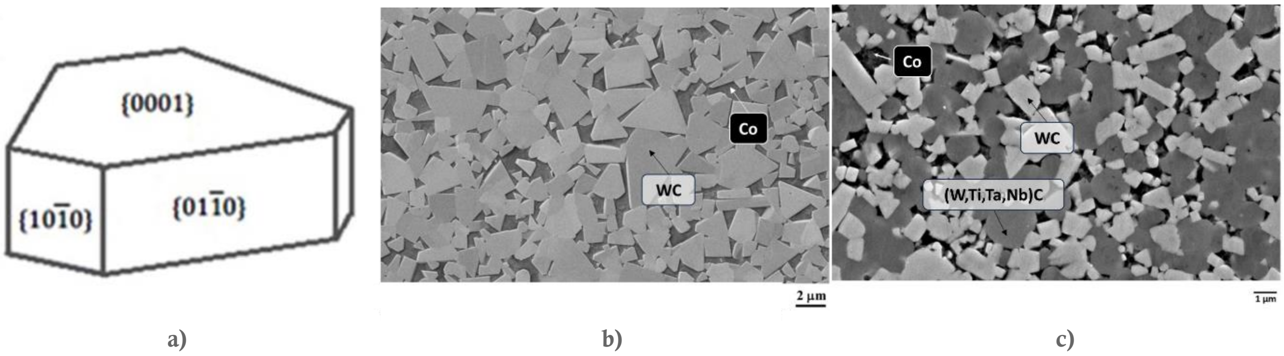

Figure 2. (a) Schematic representation of truncated WC grains shape in WC-Co composites; **(b)** a typical microstructure of WC-Co cemented carbides with microstructural parameters commonly determined for cemented carbides; **(c)** microstructure of cemented carbide with gamma phase. The light and dark phases correspond to the carbide and to the metallic binder, respectively.
Source: Adapted from Lay and Missiaen (2014), Roa *et al.* (2015) and Sandoval Ravotti *et al.* (2019).

TiC, ZrC, HfC, VC, NbC and TaC carbides are also used to produce cemented carbides. These carbides are face-centred cubic (FCC), melt congruently, and exhibit higher hardness than WC. When their content is higher than the solubility limit within the metallic binder, these elemental carbides precipitate, combining to form a mixed solid solution along with WC in the final part, which is commonly known as the cubic carbide phase or gamma (γ) phase (**Fig. 2c**); this phase is more brittle than WC. However, when their nominal content falls below the solubility limit, they behave as WC grain growth inhibitors (Exner, 1979).

Cobalt is the most used material as a metallic binder in cemented carbides. Pure Co shows an allotropic transformation from an HCP structure up to around 415 °C to a cubic structure (FCC) at higher temperatures (Davis, 1995). The prevalence of one form or another may affect the mechanical properties of the composite material. In sintered WC-Co alloys, Co shows a cubic lattice because the stabilization of it by dissolved W and C cannot be transformed by annealing (Exner, 1979; Upadhyaya, 2001).

Both the mechanical and tribological performance of cemented carbides are related to the chemical nature, amount, and size of carbide and binder phases (Chychko *et al.*, 2022; Davis, 1995; Gurland, 1988). The common parameters used to characterize the microstructure of cemented carbides are the mean grain size of the carbide particles ($d_{carbide}$) and the binder content (wt.%). The proportion of the carbide phase is generally between 3-30 wt.% of the total weight of the composite and its grain size averages between 0.4 and 10 µm.

Other important microstructural parameters are the contiguity of the carbide phase ($C_{carbide}$) and the binder's mean free path (λ_{binder}) (Exner, 1979; Roebuck and Almond, 1988; Upadhyaya, 1998), which refer to the interface area fraction of WC carbides that is shared between them and to the mean size of the metallic phase, respectively (**Fig. 2c**).

2.2. Industrial processing steps

Ammonium-para-tungstate (APT) is the usual starting raw material for standard WC powder production. After a hot reduction of the APT in hydrogen, pure tungsten powder is obtained, with controlled grain size. Tungsten and carbon are mixed in the right proportions, and this mixture is heated at high temperatures in hydrogen, forming tungsten carbide powder (Furberg *et al.*, 2019).

Different WC powder types and binders (Co, Ni) are the raw materials for the conventional manufacturing of cemented carbide, usually through a weigh-in, milling and then spray drying process.

Once the powder is ready, the production of parts follows the traditional powder metallurgy routes, either compaction plus sintering or hot compaction. Finally, the parts are finished in one or several grinding/turning/polishing steps if needed (Raihanuzzaman *et al.*, 2014).

Figure 3 shows the workflow of the entire traditional manufacturing process, starting from the APT, passing through the production of the agglomerated powder, and then compacting the part and densifying it (typically with a liquid phase sintering process). Finally, the part can be finished to provide the required surface roughness.

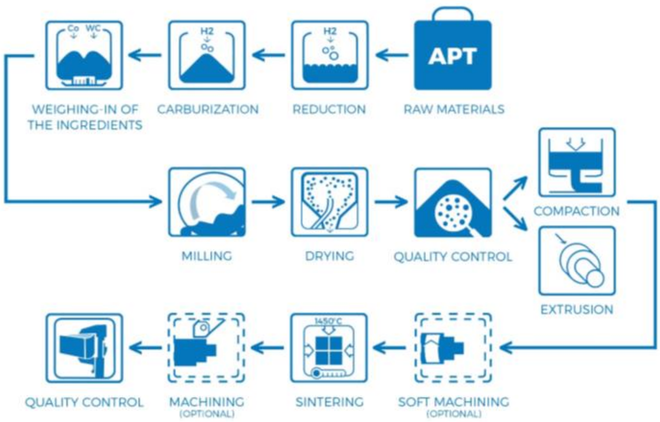

Figure 3. Traditional powder metallurgy process steps to produce parts.
Source: Adapted from Hyperion Materials & Technologies (2019).

2.3. Properties characterization

Cemented carbide products must accomplish some industrial quality checks to satisfy their demands in the application. These are related to the carbon content (through magnetic saturation measurements), carbide grain size (through coercivity values), metallographic examination, density, and hardness.

Due to the heterogeneity of cemented carbides and the cost and complexity of field testing, the development of laboratory-scale testing becomes vital for characterization of microstructure, measurement of properties and response to service-like conditions.

A wide variety of test methods according to specific standards for cemented carbides are available today (**Table 1**). Among them, hardness and fracture toughness prevail. Vickers hardness HV30 (load corresponding to 30 kg of weight), is the most used measurement. Typical values for WC–Co cemented carbides range from about 700 up to 2200 HV30. Higher values are obtained for binderless and nano–grained grades of WC–Co (Shatov *et al.*, 2014a). Finer carbide grain sizes and lower binder contents result in increased hardness, but decreased fracture toughness.

The higher the hardness, the more resistance to plastic deformation, penetration and thus abrasion wear, whereas high fracture toughness implies better absorption of impact energy by deformation, therefore, delaying crack propagation.

Hardness of cemented carbides was modelled as the sum of the in-situ hardness of the hard phase times the volume fraction of the contiguous carbide skeleton ($V_{WC}C$) and the hardness of the remaining binder times the rest of the volume (**Eq. 1**) (Shatov *et al.*, 2014a):

$$H_{CC} = H_{WC}V_{WC}C + H_{Co}(1 - V_{WC}C) \quad (1)$$

where CC denotes cemented carbides.

On the other hand, the measurement of fracture toughness in cemented carbide can be performed by several methods, with the Palmqvist test being the most accepted one. This method gives a good approximation of toughness for brittle-like cemented carbides, with a good correlation with the Chevron-notched three-point bending method from 10 to 14 MPa $m^{1/2}$. However, Palmqvist method becomes invalid when Chevron-notched three-point bending gives higher than 14 MPa $m^{1/2}$ (Sheikh *et al.*, 2015). A compilation of hardness-toughness relationship data has been recently carried out by Chychko *et al.* (2022). These authors have examined being plotted according to the microstructure, chemical composition, and processing. WC-Co data is very much dependent on particle size of WC and binder phase volume fraction, where the different grain growth inhibitors affect at a different extent the limitation of WC coarsening during conventional liquid phase sintering. The addition of cubic carbides, being present as complex solid solutions, increases the hardness but reduces the fracture toughness; high percentages of those result in cermet-like compositions. The substitution of cobalt by nickel or iron results in tendencies to high toughness/low hardness ratios and high hardness/low toughness ratios respectively. Finally, promising hardness-toughness ratios have been found by new sintering processes, but their industrialization is not yet ready.

Table 1. Standards for testing properties in cemented carbides.

Hardness	ASTM B294-22	Standard Test Method for Hardness Testing of Cemented Carbides
	ISO 3878	Hardmetals – Vickers hardness test
	ISO 3738	Hardmetals – Rockwell hardness test
	ISO 22394	Hardmetals – Knoop hardness test
Strength	ASTM B406	Standard Test Method for Transverse Rupture Strength of Cemented Carbides
	ISO 3327	Hardmetals – Determination of transverse rupture strength
Fracture toughness	ISO 28079	Hardmetals – Palmqvist toughness test
	ASTM B 771	Standard Test Method for Short Rod Fracture Toughness of Cemented Carbides
Stiffness	ISO 3312	Sintered metal materials and hardmetals – Determination of Young modulus
Wear resistance	ASTM B611	Standard Test Method for Abrasive Wear Resistance of Cemented Carbides

Note: Metallographic standards are not included here.

3. Recent advances in cemented carbides

3.1. Alternative binders

Since their discovery in 1922 by Schröter, materials with a predominant phase of WC are known preferably as cemented carbide. However, there is a variety of compositions, including binder-free and those containing TiN, that fall into the 'hardmetal' classification. Another way to refer to cemented carbides is as 'cermet,' understood as a particulate composite consisting of ceramic particles bonded with metallic matrix (German, 2005).

Co is the preferred metallic binder in cemented carbides, but provided that Co is considered carcinogenic, and both Co and W were classified by the European Union as Critical Raw Materials (Grilli *et al.*, 2017; Grohol and Veeh, 2023) (materials that are economically and strategically important for the European economy and have high risk associated with their supply), efforts have been made in the past decade to substitute it either partially or fully as a metallic binder in cemented carbides.

Although alternative binder systems have been explored since the 1980s, it is only recently that efforts have led to new materials, even more with the advances of computational systems that help tailor the properties for specific applications (Long *et al.*, 2017; Nicolás *et al.*, 2020). The most explored elements for substitution of Co are nickel (Ni) and iron (Fe) and their alloys, because they are the closest transition metals in the periodic table, and it is expected for them to have a similar affinity with carbon and tungsten as cobalt.

For applications demanding acidic corrosion resistance, Ni binder is preferred (Prakash, 2014). However, the substitution of Co is not straightforward, and an understanding of the mechanisms for microstructure formation should be well understood. In this sense, Roulon *et al.* (2020) found that for C-rich alloys, WC-Ni cemented carbides show significant grain growth with a major increase of mean intercept length and a widening of distribution, with increasing the sintering time.

In contrast, WC-Fe does not show any significant grain growth with a negligible change in the distribution of intercept length. Consequently, after 8 hours of isothermal sintering, the coarser microstructure was obtained for WC-Ni material followed by WC-Co and finally WC-Fe. In addition, in WC-Ni C-rich alloys, WC grains were more rounded, due to a more uniform precipitation of the solid on the rounded edges of the WC.

The use of alternative binders was first compiled in the review by García *et al.* (2019). Apart from exposing Ni-based and Fe-based binders as they are the closest elements to Co in the periodic table for its potential substitution, they exposed the use of: **(i)** precipitated reinforce binders for increasing hardness, wear resistance, bending strength, **(ii)** aluminide intermetallics for their high oxidation and corrosion resistance, **(iii)** High Entropy Alloys (HEA) for additionally improving hot hardness and fracture toughness, and **(iv)** ruthenium for the increase of hardness of the cemented carbide without losing the corresponding amount of toughness.

To better assess their feasibility, thermodynamic interfacial energy models between WC and liquid binder phase were proposed by Warren (1980), because this parameter is responsible for the resulting microstructure (Lay and Missiaen, 2014). The solid-liquid interfacial energy is composed by two contributing factors: the chemical contribution and the structure contribution. The last one is constant (0.31 J/m^2), as it considers only the melting point of WC grains. On the other hand, the chemical contribution is given by the binder metal, which changes as the composition of metallic alloys changes.

Long *et al.* (2017) evaluated the chemical contribution of WC-50 (Co-Ni-Al) interfacial energy at various Ni_3Al contents. The simulation showed that the chemical contribution increases from a minimum value of 0.215 J/m^2 at the composition of WC-50Co, up to 1.003 J/m^2 at the composition of WC-25Co-25Ni_3Al. Based on this information, phase diagrams can be calculated to determine the two-phase region in which a cemented carbide composed by WC and a metallic binder are the stable phases, the carbon (C) content, and the sintering temperature.

Fe- and Ni-based binders have been explored using thermodynamic simulations made with Thermo-Calc Software. Fe-Cr-Al and Fe-Ni-Cr binders showed good densification and homogeneity in agreement with simulations (Nicolás-Morillas *et al.*, 2020; 2023). Comparable or even improved combination of hardness, toughness and corrosion resistance to acidic media compared to Co binders was obtained (Nicolás-Morillas *et al.*, 2024).

Thermodynamic calculations can also help to explain variations in the grain size of the binder, which is known to be very large in comparison to the carbide phase (Mingard *et al.*, 2011). In the case of WC-50(Co-Ni-Al), alloys containing 0, 11.4 and 15.2 wt.% Ni_3Al, the grain size of the binder phase decreases as the amount of Ni_3Al increases due to the elevated driving forces for nucleation that contribute to the nuclei formation during solidification, resulting in a larger number of grains with smaller sizes (Long *et al.*, 2017). In addition, the interfacial energy between WC particles and liquid Co-Ni-Al binder becomes higher with addition of Ni_3Al, becoming an important obstacle for grain growth of the binder phase.

Another reported feature was the precipitation of the cuboidal γ' phase within the Co-Ni-Al binder, also observed in Co-Al-W superalloys (Suzuki *et al.*, 2015), which can contribute to the superior mechanical properties of the cemented carbide at elevated temperatures. Correspondingly, Konyashin *et al.* (2014; 2015) have shown that reinforced metallic binder with nanoprecipitates dramatically improves wear resistance by avoiding the detachment of the WC grains during wearing.

Besides mechanical properties, corrosion resistance and behaviour can be tailored by modifying the metallic binder. A methodical study of the corrosion behaviour of three groups of cemented carbides (WC-20 wt.% Ni, WC-20 wt.% Ni15Cr and WC-20 wt.% Ni11Cr6Mo), showed that solubility of W in Ni alloys is higher than in Co, greatly affected by the gross carbon content in the material (solubility decreases by increasing the carbon content) (Steinlechner *et al.*, 2022). For cemented carbides with low carbon i.e., high degree of alloying, WC-Ni(Cr,W) and WC-Ni(Cr, Mo, W) showed superior corrosion resistance in pH ranging from 1.5 to 7, as compared to WC-Ni(W), WC-Co(Cr, W) and WC-CoNiCr(W).

More recently, high entropy alloys (HEA) are the focus of study as substitutes for Co binder alloys. HEA are complex metallic alloys with at least five components in which any of them is principal in the composition. The advantage of using HEA is that they increase the hardness (also at elevated temperatures), fracture toughness, wear, oxidation, and corrosion resistance of cemented carbides (Straumal and Konyashin, 2023).

HEAs allow the decrease of the sintering temperature and suppress the WC grain growth during sintering (Zhou *et al.*, 2016). Refinement of WC grains is especially expected in Cr-containing compositions due to its known inhibition effect (Straumal and Konyashin, 2023). However, a two-phase material is difficult to obtain because of segregation and reaction during sintering, allowing the formation of numerous carbide phases (Mueller-Grunz *et al.*, 2019).

Despite difficulties in production of cemented carbides with HEA as binder, the improvement of properties has been demonstrated. Zhou *et al.* (2016) found an improved corrosion resistance of cemented carbides with 10 and 20 wt.% of HEA in a 0.1 M sulphuric acid solution, compared to a 10 wt.% Co material. Additionally, they found that the corrosion resistance depends only on the chemical nature of the binder and not on the binder content. Luo *et al.* (2021) found a decrease in the oxidation rate by increasing the aluminium content in the HEA binder.

Hardness and toughness have been studied more extensively. For several compositions, Zhou *et al.* (2018) found the optimal sintering temperature of 1,400°C, to obtain the highest hardness for 10 and 20 wt.% HEA cemented carbides. Moreover, when the HEA content increased to 20 wt.%, the fracture toughness increased. Dong *et al.* (2020) found that both Vickers hardness and fracture toughness increased with increasing HEA content in WC-Co materials. On the other hand, hot hardness was improved in WC-HEA, as studied by Hering *et al.* (2023).

In the work of R. Chen *et al.* (2022) they obtained increased density of WC-Co_xFeNiCrCu (x= 1, 1.5, 2, 2.5) by increasing the sintering temperature from 1,300°C up to 1450°C, with the corresponding improvement of hardness. Increasing the temperature from 1,400°C to 1,450°C promoted WC grain growth, which translated into an increase in toughness.

Comparison of hardness and fracture toughness ranges obtained for different cemented carbides with HEA as binders, with WC-10 wt.% Co, is shown in **Fig. 4**.

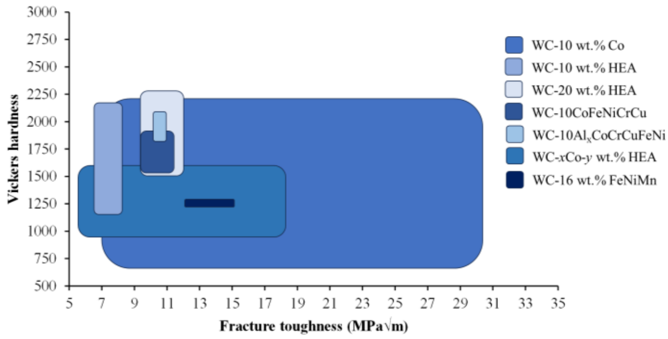

Figure 4. Vickers hardness vs. Fracture Toughness maps for cemented carbides with 10 wt.% Co, compared to cemented carbides with HEA as binders.

Source: Elaborated by the authors using the data from (García *et al.*, 2019; R. Cheng *et al.*, 2022; Dong *et al.*, 2020; Hering *et al.*, 2023; Zhou *et al.*, 2016; 2018).

3.2. New consolidation methods

Traditional powder metallurgy considers two main groups of forming technologies: cold compaction and sintering (or two-step consolidation routes) and hot compaction (or single-step consolidation routes). **Figure 5** presents the main ones for each subdivision.

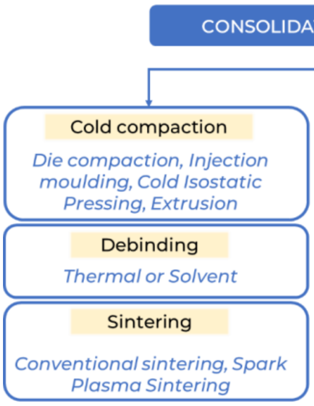

Figure 5. Main consolidation routes used for cemented carbides.

As many of these technologies have been well known for decades, the research conducted in past years has been mainly focused on two topics:

- Additive manufacturing (AM) technologies, as opposed to conventional subtractive technologies;
- Alternative sintering technologies, as opposed to conventional, time-consuming, sintering technologies, or alternative applications for well-known sintering technologies, mainly Spark Plasma Sintering (SPS).

This section will cover these two subjects. However, additionally to those, some research groups have made attempts to bring novelties on traditional technologies: micro-powder injection moulding for micro components (Heng *et al.*, 2014; Fayyaz *et al.*, 2014; 2018), casting processes using complex moulds (Kim *et al.*, 2022), or different film deposition technologies (Hu *et al.*, 2020; Xu and Huang, 2022a; 2022b; Zhao *et al.*, 2020) are examples of it.

3.2.1. Additive manufacturing technologies

The European Powder Metallurgy Association (EPMA) defines additive manufacturing as "The process of joining materials to make objects from 3D model data, usually layer upon layer, as opposed to subtractive manufacturing methodologies" (Booklet, 2019).

Conventional methodologies usually go through forming a blank that will be either green-machined, turned or ground to obtain the desired dimensions. However, these conventional approaches generate important waste and successive manufacturing operations, increasing the production cost of complex geometries.

Due to these limitations of conventional technologies, additive manufacturing provides several advantages: the agility, or capability of acting quickly without manufacturing extra tooling, the flexibility to print single parts or short series without time loss (changeover time), the creation of new complex and optimized geometries, and an important contribution to sustainability avoiding unnecessary waste (Javaid *et al.*, 2021).

There are many different additive manufacturing technologies and several ways to group them (Carreño-Morelli *et al.*, 2020; Yang *et al.*, 2020). A division that works well for cemented carbides is between one-step technologies (also called Melting Processes) and two-step technologies (or Shaping-Debinding-Sintering Processes) (**Fig. 6**) (C. Chen *et al.*, 2023).

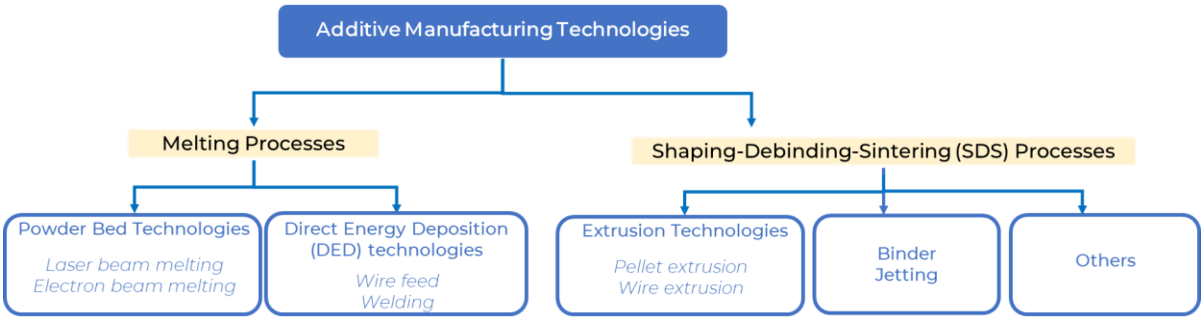

Figure 6. Metal Additive Manufacturing Technologies.

Selective Melting Processes include technologies such as Selective Laser Melting (SLM) or Electron Beam Melting (EBM) that build parts by directly melting the powder (Padmakumar, 2020). In these processes, the melting of the metallic binder is achieved in a very short time, and successive heating-cooling cycles are performed. This usually leads to many defects appearing within the structure: porosity, thermal cracks, grain growth and undesired phases, among others. Some research groups have tried alternative approaches such as higher amounts of Co, optimization of the process parameters or modification of the starting powder, but generally, these studies have not led to mechanical properties comparable to traditional powder metallurgy routes (Padmakumar, 2020; Yang *et al.*, 2020).

Shaping-Debinding-Sintering (SDS) processes are usually more suitable to process hardmetals, as the shaping/forming process is done at low temperatures and does not induce modifications within the material. The following sintering process also contributes to homogenize, remove potential defects, and fully densify the structures (Miyanaji *et al.*, 2018).

Among the different SDS processes, two have proven to give positive results for cemented carbides (WC-Co): Binder Jetting and Extrusion-Based Additive Manufacturing (see **Fig. 7**).

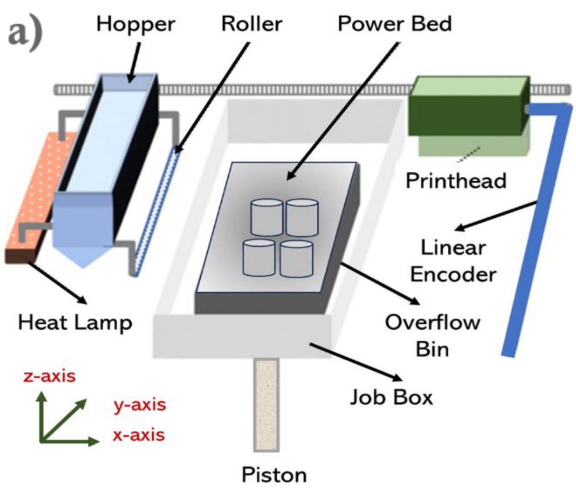

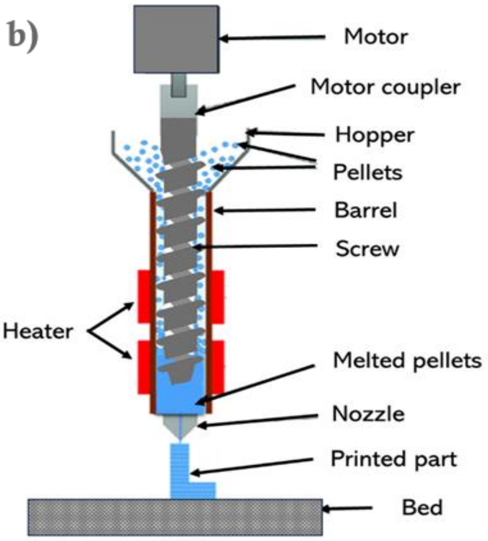

Figure 7. (a) Schematics for binder jetting technology (FFF process, Schematic of the binder-jet 3D printing machine with the printing, 2023); **(b)** extrusion-based AM (pellets extrusion process, 2023).
Source: Adapted from Gupta and Taulik (2021) and Mostafaei *et al.* (2018).

Binder Jetting is based on selectively bonding powder particles and layers together with a binder. After that, the printed parts are cured to improve the green strength and are further subjected to thermal debinding and sintering (Elliott, 2020). Studies with Co contents equal to or higher than 12wt% showed microstructures fully densified after conventional sintering processes, with medium hardnesses and acceptable wear resistances (Cramer *et al.*, 2020; Enneti and Prough, 2019; Wolfe *et al.*, 2023a; 2023b). The feedstock powder characteristics play a crucial role in the process. The possibility of using available commercial powders other than the typical ones used for additive manufacturing has been explored by Berger *et al.* (2023), finding that they can be appropriate for use in binder jetting as well.

On the other hand, extrusion-based AM technologies use as feedstock either pellets or filament manufactured with high polymer content (Altiparmak *et al.*, 2022). The principle of the technology is like commercial home printers: extruding the material (pellets or filament) through a screw and a nozzle to build the part layer-upon-layer. After the printing, the parts need to go through a debinding step (usually solvent for hardmetals) to remove one of the polymers used, then through a thermal debinding plus sintering step to eliminate the backbone binder and fully densify the parts.

These technologies have proven to obtain very good microstructures for 10% Co, although they exhibit some macroporosities due to printing limitations (Lengauer *et al.*, 2018; Yang *et al.*, 2020). An alternative to this extrusion-based AM has been developed by the Fraunhofer IKTS: Thermoplastic 3D printing (T3DP) builds the part using a precise deposition of small droplets of molten thermoplastic hard-metal-containing suspensions. After debinding and sintering, full densities were achieved, no defects were found and homogeneous microstructures were obtained (Scheithauer *et al.*, 2017; Pötschke *et al.*, 2017).

3.2.2. Alternative sintering technologies

Conventional sintering cycles are very well suited to cemented carbides and can be designed to optimize the densification of different grades. However, they also present several drawbacks:

- Time, as they tend to be long cycles, and that makes the process inefficient for short series;
- High energy consumption, leading to an important carbon footprint of these processes;
- Difficulty in sintering some alternative binders using long conventional cycles, as they might react with each other.

All those reasons lead to alternative sintering technologies being evaluated (Guillon *et al.*, 2023).

The commercial alternative technology mostly used in the past years for hardmetals is Field-assisted Sintering Technique/Spark Plasma Sintering (FAST/SPS). This technology, which has been in the market for decades, is a low-voltage, current-activated, pressure-assisted sintering process (**Fig. 8**). This combination of heating and pressure gives high heating rates and short cycle times (5–20 min), making this process very suitable for materials with low sintering activity or high reactivity (Eriksson *et al.*, 2013; Guillon *et al.*, 2014).

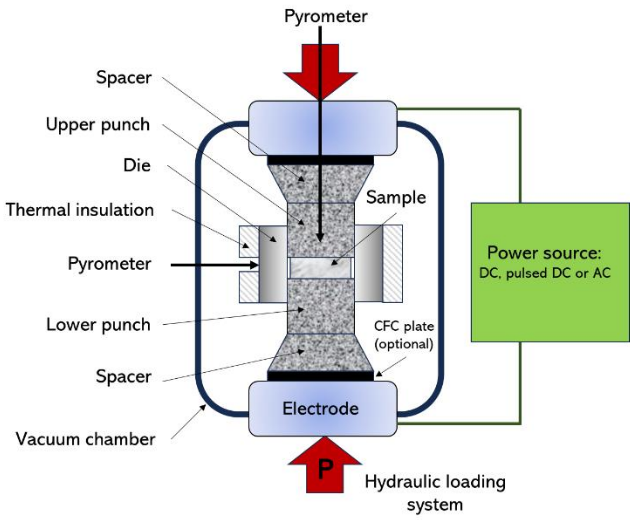

Figure 8. Schematics of the SPS process.
Source: Adapted from Bram *et al.* (2022).

Due to these characteristics, many studies have been conducted using FAST/SPS to sinter binderless powders (Tang *et al.*, 2017), nanopowders (Chuvil'deev *et al.*, 2017) or composites of tungsten carbide with other ceramics (W. Chen *et al.*, 2014; Sribalaji *et al.*, 2017; Wang *et al.*, 2018), leading to interesting results.

In recent years, some research has been dedicated to exploring additional sintering mechanisms that are not present in conventional sintering. Although the physics behind those sintering mechanisms has been shown, it is too soon to implement these processes in the industry (Guillon *et al.*, 2014; 2023). An example of these technologies is flash sintering (applying an electric field to a green body while it is heated in a conventional furnace) (Wachowicz *et al.*, 2023).

3.3. Advanced testing

Cemented carbides face such a wide array of stress-temperature-environment combinations that only a few standard parameters, as exposed in previous section 2.3, cannot describe the performance in all different applications. In terms of macroscale testing of mechanical properties, mechanical strength and abrasion wear resistance are standardized. Strength, typically measured by bending as transverse rupture (TRS), is limited by size, shape, and distribution of flaws (pore, crack, or inclusion), and by the stress distribution in the structure, i.e., the larger the body or test piece, the weaker it is since a large part has a greater chance of having a large flaw (Zak Fang *et al.*, 2014).

The abrasion resistance measured through ASTM B611 is known to be correlated with hardness following an expression of the form $V = A\ exp^{(-BH)}$, where V is the wear volume, H is the sample hardness and A and B are constants (Gee *et al.*, 2007).

Although the abrasion resistance is the only wear mode standardized for cemented carbides, it is not the only one that can be found. Other wear modes experienced by these materials are adhesive wear, fatigue, erosion, and cavitation coming from sliding, rolling, impact, fretting or slurry contacts (**Table 2**) (Beste *et al.*, 2001; Bonny *et al.*, 2010; Gee *et al.*, 2007; Lavigne *et al.*, 2022; Perez Delgado *et al.*, 2011). Typical features that result from these wear mechanisms can be binder extrusion and removal, accumulation of plastic strain in WC grains, cracking of individual WC grains and between them, and even WC grain pullout.

A compiled literature about the influence of microstructure and composition around these topics is very scarce given the many different testing parameters that can be considered in each wear test method. **Figure 9** (left side) illustrates some of the morphologic features that can be observed during those tests.

The situation becomes more complex when these mechanical requirements need to accommodate different ranges of temperatures and surrounding media. Therefore, hot hardness, oxidation, creep, and corrosion, as well as wear-corrosion synergy effects have been tested (Boukantar *et al.*, 2021; Fathipour *et al.* 2024; Gant *et al.*, 2004; Guo *et al.* 2018; Lebedev *et al.* 2023; Maier *et al.* 2021; Tang *et al.*, 2023). All these properties are generally evaluated according to the microstructural parameters and binder nature.

Table 2. General standards used to test wear in cemented carbides.

Standard ref	Test
ASTM G65	Standard Test Method for Measuring Abrasion Using the Dry Sand/Rubber Wheel Apparatus
ASTM G133	Standard Test Method for Linearly Reciprocating Ball-on-Flat Sliding Wear
ASTM G99	Standard Test Method for Wear Testing with a Pin-on-Disk Apparatus
ASTM G32	Standard Test Method for Cavitation Erosion Using Vibratory Apparatus
ASTM-G76	Standard Test Method for Conducting Erosion Tests by Solid Particle Impingement Using Gas Jets

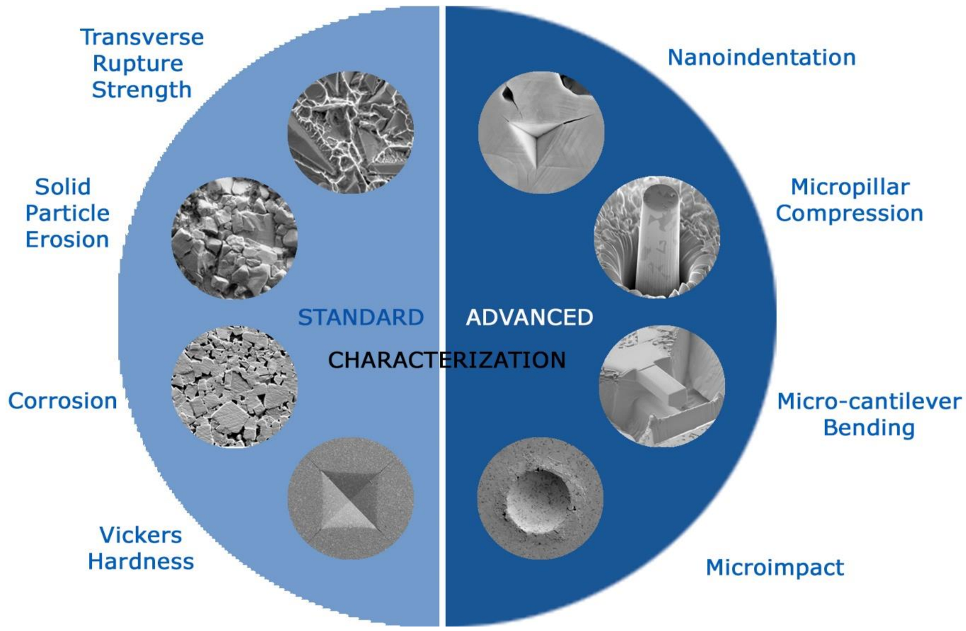

Figure 9. Some morphological features from cemented carbides tested in different conditions; left (standard) and right (advanced) characterization techniques.

Source: Elaborated by the authors using data from Cinca *et al.* (2019), Ortiz-Membrado *et al.* (2021), Sandoval Ravotti (2019), Hyperion Materials & Technologies (2019).

Due to the cost and time-consuming efforts to provide complete characterization, and to facilitate new materials development, machine learning strategies have also been introduced in this sector (Guan *et al.*, 2022). However, their use is not yet of widespread knowledge.

Interestingly, many of the material developments have been linked and helped by emerging advanced testing and characterization methods that appear due to the necessity in materials science to further explore connections between microstructure and bonding with final properties. Hence, in recent years, the use of conventional techniques has been complemented with the use of more sophisticated ones working at the micro and nanoscale.

The understanding of the material performance at small scales is important because the mechanical failure of any bulk material is triggered by the formation, extension, or local accumulation of initial small defects (Naughton-Duszová *et al.*, 2019). Specifically for cemented carbides, classical works focused on the intergranular and intragranular fracture of WC grains, the formation and rupture of Co ligaments and the decohesion of the Co-WC interface, even on crack propagation and plastic deformation of the binder.

In recent years, 3D visualization techniques, such as serial sectioning, Focused Ion Beam /Field Emission Scanning Electron Microscopy (FIB/FESEM) Tomography, X-ray tomography, Transmission Electron Microscopy (TEM) based tomography and atom probe tomography are becoming helpful in providing images of the internal structures, specifically on the spatial distribution of phases, real feature shapes and sizes, and feature connectivity. The FIB/FESEM tomography has been used by some scientists to reveal the complexity of the WC carbide skeleton and binder ligaments in cemented carbides to study crack propagation (Jiménez-Piqué *et al.*, 2017; Tarragó *et al.*, 2015).

Nanoindentation is the most appropriate technique to determine mechanical properties such as hardness and elastic modulus for the constitutive phases. However, intrinsic response of constitutive phases is usually not considered in the overall behavior of the composite material. For example, it has been established that hardness of WC is anisotropic (Naughton-Duszová *et al.*, 2013; Roebuck *et al.*, 2012), with hardness values for WC basal planes significantly higher than for the prismatic orientation.

Focused ion-beam (FIB) has also been used to investigate the morphological features below local phase nanoindentations (Walbrühl *et al.*, 2018). Electron Backscattered Diffraction (EBSD), Scanning Electron Microscopy (SEM) and Atomic Force Microscopy (AFM) have been used to evaluate the dependence of hardness and deformation mechanisms on orientation for WC grains in coarse WC-Co materials (Csanádi *et al.*, 2015).

Furthermore, binder is a Co-W-C alloy in which the amount of the alloying elements plays an important role on the intrinsic hardness and deformation mechanisms. On the other hand, disposition of the surrounding carbide particles, i.e., constraint degree, affects its flow stress in the composite (Roa *et al.*, 2016). All these measurements have been lately complemented by the statistical analysis provided in massive nanoindentation studies on the small scale, reporting hardness values for Co-based binder of around 8 GPa constrained by the WC grains. Around 30 GPa and 22 GPa were measured for the basal and prismatic WC planes, respectively (Roa *et al.*, 2015).

Walbrühl *et al.* (2018) studied thoroughly the hardness of an alternative Ni-based binder in cemented carbides (85Ni15Fe alloy). In their study, they assessed the effect of the WC particles surrounding the indentation made in the metallic binder. According to their results, the measured hardness of the metallic binder first should be corrected to neglect the pile-up effect found in Ni alloys. Moreover, the measured hardness increases with the proximity of WC particles to the indentation, obtaining the maximum value when the indentation touches a carbide particle. After correction, intrinsic hardness of the metallic binder approximates its value, to that of a bulk alloy with similar composition. Such finding is critical as input for FEM simulations.

Regarding small scale, many studies have found estimated data in agreement with experimental data by assuming an effect of the length scale, such as a Hall-Petch relationship in intrinsic hardness of constitutive phases, regardless the constrain factors (Shatov *et al.*, 2014b; Xu and Ågren, 2004). Besides nanoindentation, uniaxial compression of micropillars gives further insights on the local response of cemented carbides.

Samples for uniaxial compression of micropillars are micron-sized pillars prepared by FIB milling. Micropillars are afterwards deformed with a nanoindenter equipped with a flat punch. The failure initiation at WC/Co and WC/WC has been investigated according to the specimen size through in-situ uniaxial compression and FESEM microscopy. Different mechanical responses depend on the ratio of the WC grain size and micropillar diameter (Csanádi *et al.*, 2014; Sandoval Ravotti *et al.*, 2018; 2019).

Material deformation and fracture have also been examined by micro-beam bending through free-standing micro-cantilevers, where also the specimen size is of importance (Csanádi *et al.*, 2020; Elizalde *et al.*, 2018; Klünsner *et al.*, 2011; Ortiz-Membrado *et al.*, 2021; Trueba *et al.*, 2014). Load vs. displacement curves have been reported with the analysis of fractographic behaviours. The technique has contributed to evaluating the role of individual microstructural features in cemented carbides (single WC crystals and single Co ligaments as well as WC/WC and WC/Co boundaries) (Csanádi *et al.*, 2020; Trueba *et al.*, 2014). An average mechanical strength of 6.32 GPa for ultrafine specimens with 8.2 wt.% Co content and 5.46 Gpa for those with 12 wt.% Co content were found (Klünsner *et al.*, 2011). Fracture strength values as high as 20-25 Gpa for WC/WC boundaries in a 6.5 wt.% Co coarse cemented carbide were found (Elizalde *et al.*, 2018). Also, in a coarse specimen but with 16.7 vol.% Co, most of the WC/WC boundaries exhibited brittle failure with an average fracture strength of 4.1 ± 2.5 GPa (Csanádi *et al.*, 2020). Fracture toughness of single WC grains has been also assessed as 5.6 ± 0.8 $MPa \cdot m^{1/2}$ by means of the micro-beam bending technique (Ortiz-Membrado *et al.*, 2021).

Additionally, the use of spherical indenters for monotonic and cyclic Hertzian indentation loading has attracted attention with the aim to evaluate plastic deformation features beneath the indenter as well as residual strength.

In the last years, monotonic loading has been used to evaluate the damage tolerance of cemented carbides, i.e., deformation prevailing over fracture as damage mode. This allows the optimization of the microstructural design to improve reliability by mapping the transition from brittle to quasi-plastic damage (Góez *et al.*, 2012; Mahani *et al.*, 2024). On the other hand, the use of cyclic loading is useful to evaluate fatigue sensitivity.

The use of macro, micro and nano-scale impact tests have been useful to test WC-Co specimens with thin coatings where the ratio of coating thickness *t* to the indenter radius *R* (t/R), has been explored. Deformation and failure mechanisms depend on applied load and indenter sharpness (Beake, 2022). In nano-impact test for coated specimens, due to force limitations, very sharp probes are used, which can break eventually if testing tough materials. Micro-impact tests (repetitive loads at 1-3N) have been used to avoid probe damage. This test is severe/accelerated even at low forces, and it is an "in situ" test where the impact damage is followed cycle by cycle.

Deformation and cracking of uncoated cemented carbides has been found to be dependent on the H/E and H^3/E^2 ratios (H being the hardness and E the elastic modulus), known as the elastic strain to break and the resistance to plastic deformation, respectively (Cinca *et al.*, 2019).

Wear at the micro and nanoscale also has been examined in the last decade by means of scratch testing. Diamond indenters with different radii have been used while applying different loads and sliding speeds. The friction coefficient is systematically recorded, and the damage mechanisms examined. Intergranular and intragranular WC cracking as well as at WC-Co interfaces have been found (Gee *et al.*, 2017; Gee and Nimishakavi, 2011). As it can be defined as an abrasion wear mode, it has been also found that smaller WC grain sizes lead to better wear resistance.

The same methodology as in a scratch test but with different stylus material has been used to evaluate adhesive wear, concluding that submicrometric surface irregularities have more influence than carbide composition on metal transfer (Olsson and Cinca, 2024).

Finally, nanoindentation, scratch and contact damage tests in aggressive media show evidence of corrosion effects (by removal of the metallic binder) in the mechanical integrity of cemented carbides (Gant *et al.*, 2013; Zheng *et al.*, 2019; 2022a; 2022b). **Figure 9** (right side) illustrates features of tested cemented carbides by means of those micromechanical characterization methods above described.

4. Concluding remarks

Within these 100 years of existence for cemented carbides, progress on new formulations and processing methods has been made. However, the last decade has witnessed an increased challenge given the necessity of substituting Co, not only due to its carcinogenic effects, but to its consideration as a critical raw material by the European Union.

With the necessity to assist more demanding applications, academic and industrial experts have extensively worked to overcome these potential challenges. This has resulted in increased publications where High Entropy Alloys (HEAs) have been explored due to their high hardness at elevated temperatures in addition to high wear and corrosion resistance.

Moreover, the boom in additive manufacturing technologies and the application of Spark Plasma Sintering or Field-assisted Sintering Technique (FAST/SPS) to sinter binderless powders, nanopowders or composites of tungsten carbide with other ceramics has opened new possibilities.

Finally, new, and advanced characterization techniques such as nanoindentation, compression of micropillars and micro-beam bending through free-standing micro-cantilevers, are helping to provide insights into the mechanical properties of cemented carbides and their constitutive phases.

Authors' contributions

Conceptualization: Sandoval Ravotti, D. S.; Melero, H.; Cinca, N.; **Data collection:** Not applicable; **Formal Analysis:** Not applicable; **Funding acquisition:** Not applicable; **Investigation:** Not applicable; **Methodology:** Not applicable; **Project administration:** Not applicable; **Resources:** Not applicable; **Software:** Not applicable; **Supervision:** Cinca, N.; **Validation:** Not applicable; **Visualization:** Not applicable; **Writing – original draft:** Sandoval Ravotti, D. S.; Melero, H.; Cinca, N.; **Writing – review & editing:** Sandoval Ravotti, D. S.; Melero, H.; Cinca, N.

Data availability statement

Data sharing is not applicable.

Funding

Not applicable.

Acknowledgments

The authors want to acknowledge the marketing team at Hyperion Materials and Technologies for providing editing help of internal pictures.

References

Altıparmak, S. C.; Yardley, V. A.; Shi, Z.; Lin, J. Extrusion-based additive manufacturing technologies: State of the art and future perspectives. *J. Manufact. Proc.* **2022**, 83, 607–636. https://doi.org/10.1016/j.jmapro.2022.09.032

Beake, B. D. Nano- and Micro-Scale Impact Testing of Hard Coatings: A Review. *Coatings.* **2022**, *12* (6), 793. https://doi.org/10.3390/COATINGS12060793

Berger, C.; Pötschke, J.; Scheithauer, U.; Michaelis, A. Correlation of Different Cemented Carbide Starting Powders with the Resulting Properties of Components Manufactured via Binder Jetting. *Metals.* **2023**, *13*, 1848. https://doi.org/10.3390/met13111848

Beste, U.; Hammerström, L.; Engqvist, H.; Rimlinger, S.; Jacobson S. Particle erosion of cemented carbides with low Co content. *Wear*. **2001**, *250* (1–12), 809–817. https://doi.org/10.1016/S0043-1648(01)00735-9

Bonny, K.; De Baets, P.; Quintelier, J.; Vleugels, J.; Jiang, D.; VanderBiest, O.; Lauwers, B.; Liu, W. Surface finishing: Impact on tribological characteristics of WC–Co hardmetals. *Tribol. Int.* **2010**, *43* (1–2), 40–54. https://doi.org/10.1016/j.triboint.2009.04.029

Booklet. *ADDITIVE MANUFACTURING TECHNOLOGY A Guide for Designers and Engineers.* EPMA, 2019. https://www.epma.com/european-additive-manufacturing-group (accessed 2024-01-01).

Boukantar, A. R.; Djerdjare, B.; Guiberteau, F.; Ortiz, A. L. A Critical Comparison of the Tribocorrosive Performance in Highly-Alkaline Wet Medium of Ultrafine-Grained WC Cemented Carbides with Co, Co+Ni, or Co+Ni+Cr Binders. *Int. J. Refract. Metals Hard Mater.* **2021**, *95*, 105452. https://doi.org/10.1016/j.ijrmhm.2020.105452

Bram, M.; Beynet, Y.; Van Der Laan, A.; Neubauer, E.; Guillon, O.; Huber, J.; Trapp, J.; Keszler, M.; Luthardt, B.; Hennicke, J. *Introduction to Field-Assisted Sintering Technology/Spark Plasma Sintering (FAST/SPS)*; 2022.

Carreño-Morelli, E.; Alveen, P.; Moseley, S.; Rodriguez-Arbaizar, M.; Cardoso, K. Three-Dimensional Printing of Hard Materials. *Int. J. Refract. Metals Hard Mater.* **2020**, *87*, 105110. https://doi.org/10.1016/j.ijrmhm.2019.105110

Chen, W. H.; Lin, H. T.; Nayak, P. K.; Huang, J. L. Material Properties of Tungsten Carbide-Alumina Composites Fabricated by Spark Plasma Sintering. *Ceram. Int.* **2014**, *40* (9 PART B), 15007–15012. https://doi.org/10.1016/j.ceramint.2014.06.102

Chen, R.; Zheng, S.; Zhou, R.; Wei, B.; Yang, G.; Chen, P.; Cheng, J. Development of Cemented Carbides with CoxFeNiCrCu High-Entropy Alloyed Binder Prepared by Spark Plasma Sintering. *Int. J. Refract. Metals Hard Mater.* **2022**, *103*, 105751. https://doi.org/10.1016/J.IJRMHM.2021.105751

Chen, C.; Huang, B.; Liu, Z.; Li, Y.; Zou, D.; Liu, T.; Chang, Y.; Chen, L. Additive Manufacturing of WC-Co Cemented Carbides: Process, Microstructure, and Mechanical Properties. *Additive Manufacturing*. **2023**, *63*, 103410. https://doi.org/10.1016/j.addma.2023.103410

Chuvil'deev, V. N.; Blagoveshchenskiy, Y. V.; Nokhrin, A. V.; Boldin, M. S.; Sakharov, N. V.; Isaeva, N. V.; Shotin, S. V.; Belkin, O. A.; Popov, A. A.; Smirnova, E. S.; Lantsev, E. A. Spark Plasma Sintering of Tungsten Carbide Nanopowders Obtained through DC Arc Plasma Synthesis. *J. Alloys Compd.* **2017**, *708*, 547–561. https://doi.org/10.1016/j.jallcom.2017.03.035

Chychko, A.; García, J.; Collado Ciprés, V.; Holmström, E.; Blomqvist, A. HV-KIC Property Charts of Cemented Carbides: A Comprehensive Data Collection. *Int. J. Refract. Metals Hard Mater.* **2022**, *103*, 105763. https://doi.org/10.1016/j.ijrmhm.2021.105763

Cinca, N.; Beake, B. D.; Harris, A. J.; Tarrés, E. Micro-Scale Impact Testing on Cemented Carbides. *Int. J. Refract. Metals Hard Mater.* **2019**, *84*, 105045. https://doi.org/10.1016/J.IJRMHM.2019.105045

Cramer, C. L.; Aguirre, T. G.; Wieber, N. R.; Lowden, R. A.; Trofimov, A. A.; Wang, H.; Yan, J.; Paranthaman, M. P.; Elliott, A. M. Binder Jet Printed WC Infiltrated with Pre-Made Melt of WC and Co. *Int. J. Refract. Metals Hard Mater.* **2020**, *87*, 105137. https://doi.org/10.1016/j.ijrmhm.2019.105137

Csanádi, T.; Bl'anda, M.; Naughton-Duszová, A.; Chinh, N. Q.; Szommer, P.; Dusza, J. Deformation Characteristics of WC Micropillars. *J. Eur. Ceram. Soc.* **2014**, *34* (15), 4099–4103. https://doi.org/10.1016/J.JEURCERAMSOC.2014.05.045

Csanádi, T.; Bl'Anda, M.; Chinh, N. Q.; Hvizdoš, P.; Dusza, J. Orientation-Dependent Hardness and Nanoindentation-Induced Deformation Mechanisms of WC Crystals. *Acta Mater.* **2015**, *83*, 397–407. https://doi.org/10.1016/J.ACTAMAT.2014.09.048

Csanádi, T.; Vojtko, M.; Dusza, J. Deformation and Fracture of WC Grains and Grain Boundaries in a WC-Co Hardmetal during Microcantilever Bending Tests. *Int. J. Refract. Metals Hard Mater.* **2020**, *87*, 105163. https://doi.org/10.1016/J.IJRMHM.2019.105163

Davis, J. R. *ASM Specialty Handbook:* Tool Materials; ASM International, 1995.

Dong, D.; Xiang, X.; Huang, B.; Xiong, H.; Zhang, L.; Shi, K.; Liao, J. Microstructure and Properties of WC-Co/CrMnFeCoNi Composite Cemented Carbides. *Vacuum.* **2020**, *179*, 109571. https://doi.org/10.1016/J.VACUUM.2020.109571

Elizalde, M. R.; Ocaña, I.; Alkorta, J.; Sánchez-Moreno, J. M. Mechanical Strength Assessment of Single WC-WC Interfaces Present in WC-Co Hardmetals through Micro-Beam Bending Experiments. *Int. J. Refract. Metals Hard Mater.* **2018**, *72*, 39–44. https://doi.org/10.1016/J.IJRMHM.2017.12.009

Elliot, A.; Cramer, C.; Nandwana, P. *Binder Jetting and Sintering in Additive Manufacturing*; USDOE Office of Energy Efficiency and Renewable Energy (EERE), 2020. https://doi.org/10.31399/asm.hb.v24.a0006569

Enneti, R. K.; Prough, K. C. Wear Properties of Sintered WC-12%Co Processed via Binder Jet 3D Printing (BJ3DP). *Int. J. Refract. Metals Hard Mater.* **2019**, *78*, 228–232. https://doi.org/10.1016/j.ijrmhm.2018.10.003

Eriksson, M.; Radwan, M.; Shen, Z. Spark Plasma Sintering of WC, Cemented Carbide and Functional Graded Materials. *Int. J. Refract. Metals Hard Mater.* **2013**, *36*, 31–37. https://doi.org/10.1016/j.ijrmhm.2012.03.007

Ettmayer, P.; Kolaska, H.; Ortner, H. M. History of Hardmetals. In *Comprehensive Hard Materials Vol. 1-3*; Sarin, V.; Mari, D.; Llanes, L.; Nebel, C. E., Eds.; Elsevier, 2014; pp 3–27. https://doi.org/10.1017/CBO9781107415324.004

Exner, H. E. Physical and Chemical Nature of Cemented Carbides. *Int. Mat. Rev.* **1979**, *4*, 1149–1173. https://doi.org/10.1179/imtr.1979.24.1.149

Fathipour, Z.; Hadi, M.; Maleki, M.R.; Fernandes, F. Effect of Binder on Oxidation Properties of Tungsten Carbides: A Review by a Conceptual Classification Approach. *Ceramics.* **2024**, *7*, 166–191. https://doi.org/10.3390/ceramics7010011

Fayyaz, A.; Muhamad, N.; Sulong, A. B.; Rajabi, J.; Wong, Y. N. Fabrication of Cemented Tungsten Carbide Components by Micro-Powder Injection Moulding. *J. Mater. Process Technol.* **2014**, *214* (7), 1436–1444. https://doi.org/10.1016/j.jmatprotec.2014.02.006

Fayyaz, A.; Muhamad, N.; Sulong, A. B. Microstructure and Physical and Mechanical Properties of Micro Cemented Carbide Injection Moulded Components. *Powder Technol.* **2018**, *326*, 151–158. https://doi.org/10.1016/j.powtec.2017.12.011

Furberg, A.; Arvidsson, R.; Molander, S. Environmental Life Cycle Assessment of Cemented Carbide (WC-Co) Production. *J. Clean Prod.* **2019**, *209*, 1126–1138. https://doi.org/10.1016/j.jclepro.2018.10.272

Gant, A. J.; Gee, M. G.; May, A. T. The Evaluation of Tribo-Corrosion Synergy for WC-Co Hardmetals in Low Stress Abrasion. *Wear.* **2004**, *256* (5), 500–516. https://doi.org/10.1016/j.wear.2003.04.001

Gant, A. J.; Gee, M. G.; Gohil, D. D.; Jones, H. G.; Orkney, L. P. Use of FIB/SEM to Assess the Tribo-Corrosion of WC/Co Hardmetals in Model Single Point Abrasion Experiments. *Tribol. Int.* **2013**, *68*, 56–66. https://doi.org/10.1016/J.TRIBOINT.2012.11.008

García, J.; Collado Ciprés, V.; Blomqvist, A.; Kaplan, B. Cemented Carbide Microstructures: A Review. *Int. J. Refract. Metals Hard Mater.* **2019**, *80*, 40–68. https://doi.org/10.1016/j.ijrmhm.2018.12.004

Gee, M. G.; Gant, A.; Roebuck, B. Wear Mechanisms in Abrasion and Erosion of WC / Co and Related Hardmetals. *Wear.* **2007**, *263*, 137–148. https://doi.org/10.1016/j.wear.2006.12.046

Gee, M. G.; Nimishakavi, L. Model Single Point Abrasion Experiments on WC/Co Hardmetals. *Int. J. Refract. Metals Hard Mater.* **2011**, *29* (1), 1–9. https://doi.org/10.1016/J.IJRMHM.2010.04.009

Gee, M.; Mingard, K.; Nunn, J.; Roebuck, B.; Gant, A. In Situ Scratch Testing and Abrasion Simulation of WC/Co. *Int. J. Refract. Metals Hard Mater.* **2017**, *62*, 192–201. https://doi.org/10.1016/J.IJRMHM.2016.06.004

German, R. M. *A-Z of Powder Metallurgy*; Elsevier, 2005.

Góez, A.; Coureaux, D.; Ingebrand, A.; Reig, B.; Tarrés, E.; Mestra, A.; Mateo, A.; Jiménez-Piqué, E.; Llanes, L. Contact damage and residual strength in hardmetals, *Int. J. Refract. Metals Hard Mater.* **2012**, *30*, 121–127. https://doi.org/10.1016/j.ijrmhm.2011.07.013

Grilli, M. L.; Bellezze, T.; Gamsjäger, E.; Rinaldi, A.; Novak, P.; Balos, S.; Piticescu, R. R.; Ruello, M. L. Solutions for Critical Raw Materials under Extreme Conditions: A Review. *Materials.* **2017**, *10*, 285. https://doi.org/10.3390/ma10030285

Grohol, M; Veeh, C. *Study on the Critical Raw Materials for the EU 2023*; European Comission, 2023. https://op.europa.eu/en/publication-detail/-/publication/57318397-fdd4-11ed-a05c-01aa75ed71a1 (accessed 2024-01-01).

Guan, Z.; Li, N.; Zhang, W.; Wang, J.; Wang, C.; Shen, Q.; Xu, Z.; Peng, J.; Du, Y. A Multiple Loops Machine Learning Framework to Predict the Properties of WC–Co Based Cemented Carbides. *Int. J. Refract. Metals Hard Mater.* **2022**, *104*, 105798. https://doi.org/10.1016/j.ijrmhm.2022.105798

Guillon, O.; Gonzalez-Julian, J.; Dargatz, B.; Kessel, T.; Schierning, G.; Räthel, J.; Herrmann, M. Field-Assisted Sintering Technology/Spark Plasma Sintering: Mechanisms, Materials, and Technology Developments. *Adv. Eng. Mater.* **2014**, *16* (7), 830–849. https://doi.org/10.1002/adem.201300409

Guillon, O.; Rheinheimer, W.; Bram, M. A Perspective on Emerging and Future Sintering Technologies of Ceramic Materials. *Adv. Eng. Mater.* **2023**, *25*, 2201870. https://doi.org/10.1002/adem.202201870

Guo, B.; Zhang, L.; Cao, L.; Zhang, T.; Jiang, F.; Yan, L. The Correction of Temperature-Dependent Vickers Hardness of Cemented Carbide Base on the Developed High-Temperature Hardness Tester. *J. Mater. Process Technol.* **2018**, *255*, 426–433. https://doi.org/10.1016/J.JMATPROTEC.2017.12.041

Gupta, A. K.; Taulik, M. Effect of Process Variables on Performances Measured in Filament and Pellet Based Extrusion Processes. *Materials Today.* **2021**, *47* (15) 5177–5184. https://doi.org/10.1016/j.matpr.2021.05.508

Gurland, J. New scientific approaches to development of tool materials. *Int. Mater. Rev.* **1988**, *33* (1), 151–166. https://doi.org/10.1179/imr.1988.33.1.151

Heng, S. Y.; Raza, M. R.; Muhamad, N.; Sulong, A. B.; Fayyaz, A. Micro-Powder Injection Molding (MPIM) of Tungsten Carbide. *Int. J. Refract. Metals Hard Mater.* **2014**, *45*, 189–195. https://doi.org/10.1016/j.ijrmhm.2014.04.012

Hering, B.; Gestrich, T.; Steinborn, C.; Vornberger, A.; Pötschke, J. Influence of Alternative Hard and Binder Phase Compositions in

Hardmetals on Thermophysical and Mechanical Properties. *Metals*. **2023**, *13*, 1803. https://doi.org/10.3390/met13111803

Hu, D.; Liu, Y.; Chen, H.; Wang, M. Microstructure and Wear Resistance of Ni-Based Tungsten Carbide Coating by Laser Cladding on Tunnel Boring Machine Cutter Ring. *Surf. Coat. Technol.* **2020**, *404*, 126432. https://doi.org/10.1016/j.surfcoat.2020.126432

Hyperion Materials & Technologies. *All about cemented carbide*. http://www.allaboutcementedcarbide.com/ (accessed 2019-08-22).

Javaid, M.; Haleem, A.; Singh, R.; Suman, R.; Rab, S. Role of additive manufacturing applications towards environmental sustainability. *Adv. Ind. Eng. Polym. Res*. **2021**, *4* (4), 312. https://doi.org/10.1016/j.aiepr.2021.07.005

Jiménez-Piqué, E.; Turon-Vinas, M.; Chen, H.; Trifonov, T.; Fair, J.; Tarrés, E.; Llanes, L. Focused ion beam tomography of WC-Co cemented carbides, *Int. J. Refract. Metals Hard Mater.* **2017**, *67*, 9–17. https://doi.org/10.1016/j.ijrmhm.2017.04.007

Kim, H.; Kim, J. I.; Ryu, S. S.; Jeong, H. Cast WC-Co Alloy-Based Tool Manufacturing Using a Polymeric Mold Prepared via Digital Light Processing 3D Printing. *Mater. Lett.* **2022**, *306*. https://doi.org/10.1016/j.matlet.2021.130979

Klünsner, T.; Wurster, S.; Supancic, P.; Ebner, R.; Jenko, M.; Glätzle, J.; Püschel, A.; Pippan, R. Effect of specimen size on the tensile strength of WC–Co hard metal. *Acta Mater.* **2011**, *59*, 4244–4252. https://doi.org/10.1016/j.actamat.2011.03.049

Konyashin, I.; Lachmann, F.; Ries, B.; Mazilkin, A.; Straumal, B.; Kübel, C.; Llanes, L.; Baretzky, B. Strengthening Zones in the Co Matrix of WC–Co Cemented Carbides. *Scr Mater* **2014**, *83*, 17–20. https://doi.org/10.1016/J.SCRIPTAMAT.2014.03.026

Konyashin, I.; Ries, B.; Hlawatschek, D.; Zhuk, Y.; Mazilkin, A.; Straumal, B.; Dorn, F.; Park, D. Wear-Resistance and Hardness: Are They Directly Related for Nanostructured Hard Materials? *Int. J. Refract. Metals Hard Mater.* **2015**, *49* (1), 203–211. https://doi.org/10.1016/J.IJRMHM.2014.06.017

Konyashin, I. Approaching the 100th Anniversary of the Hardmetal Invention: From First WC-Co Samples towards Modern Advanced Hardmetal Grades. *Int. J. Refract. Metals Hard Mater.* **2023**, *111*, 106113. https://doi.org/10.1016/J.IJRMHM.2023.106113

Lavigne, O.; Cinca, N.; Ther, O.; Tarrés, E. Effect of Binder Nature and Content on the Cavitation Erosion Resistance of Cemented Carbides. *Int. J. Refract. Metals Hard Mater.* **2022**, *109*, 105978. https://doi.org/10.1016/j.ijrmhm.2022.105978

Lay, S.; Missiaen, J. M. Microstructure and Morphology of Hardmetals. In *Comprehensive Hard Materials*; Sarin, V. K., Mari, D., Llanes, L., Nebel, C. E., Eds.; Elsevier, 2014; pp 91–117.

Lebedev, A.; Alves, N.; Balbino, N.; Otoni Corrêa, E.; Roque Huanca, D.; Amaury De Freitas Matos, F.; De Carvalho Valeriano, L. Comparative Study of Corrosion Behaviors of WC-NiMo and WC-Co Cemented Carbides. *Materials.* **2023**, *16* (12), 4480. https://doi.org/10.3390/MA16124480

Lengauer, W.; Kukla, C.; Kitzmantel, M.; Duretek, I.; Schwarz, V.; Neubauer, E.; Lieberwirth, C.; Morrison, V. Preparation and properties of extrusion-based 3D-printed hardmetal and cermet parts. In: *Proceedings of the Euro PM2018 Congress & Exhibition Euro PM2018 Proceedings, Bilbao Exhibition Centre (BEC)*, Bilbao, Spain. 2018. p. 14-18.

Long, J.; Zhang, W.; Wang, Y.; Du, Y.; Zhang, Z.; Lu, B.; Cheng, K.; Peng, Y. A New Type of WC–Co–Ni–Al Cemented Carbide: Grain Size and Morphology of Γ′-Strengthened Composite Binder Phase. *Scr. Mater.* **2017**, *126*, 33–36. https://doi.org/10.1016/j.scriptamat.2016.08.007

Luo, W.; Liu, Y.; Liu, X.; Zhou, Z. Oxidation behavior of ultrafine WC-based cemented carbides with AlxCoCrCuFeNi high-entropy alloy binders. *Ceram. Intern*. **2021**, *47*, 8498–8509. https://doi.org/10.3390/met13010171

Mahani, F.; Liu, C.; Sousa Machado, P. V.; Lin, L. L.; Wen, X.; Jiménez-Piqué, E.; Llanes, L.; Contact damage induced by means of conical indentation in hardmetals: Microstructural effects on residual strength. *Int. J. Refract. Metals Hard Mater.* **2024**, *118*, 106446, https://doi.org/10.1016/j.ijrmhm.2023.106446

Maier, K.; Klünsner, T.; Krobath, M.; Pichler, P.; Marsoner, S.; Ecker, W.; Czettl, C.; Schäfer, J.; Ebner, R. Creep Behaviour of WC-12 Wt% Co Hardmetals with Different WC Grain Sizes Tested in Uniaxial Tensile and Compression Step-Loading Tests at 700 °C and 800 °C. *Int. J. Refract. Metals Hard Mater.* **2021**, *100*, 105633. https://doi.org/10.1016/J.IJRMHM.2021.105633

Mingard, K. P.; Roebuck, B.; Marshall, J.; Sweetman, G. Some Aspects of the Structure of Cobalt and Nickel Binder Phases in Hardmetals. *Acta Mater.* **2011**, *59* (6), 2277–2290. https://doi.org/10.1016/J.ACTAMAT.2010.12.004

Miyanaji, H.; Orth, M.; Akbar, J. M.; Yang, L. Process Development for Green Part Printing Using Binder Jetting Additive Manufacturing. *Front. Mech. Eng*. **2018**, *13*, 504–512. https://doi.org/10.1007/s11465-018-0508-8

Mostafaei, A.; Neelapu, S. H. V. R.; Kisailus, C.; Nath, L. M.; Jacobs, T. D. B.; Chmielus, M. Characterizing surface finish and fatigue behavior in binder-jet 3D-printed nickel-based superalloy 625. *Additive Manufacturing*. **2018**, *24*, 200–209. https://doi.org/10.1016/j.addma.2018.09.012

Mueller-Grunz, A.; Alveen, P.; Rassbach, S.; Useldinger, R.; Moseley, S. The Manufacture and Characterization of WC-(Al)CoCrCuFeNi Cemented Carbides with Nominally High Entropy Alloy Binders. *Int. J. Refract. Metals Hard Mater.* **2019**, *84*, 105032. https://doi.org/10.1016/j.ijrmhm.2019.105032

Naughton-Duszová, A.; Csanádi, T.; Sedlák, R.; Hvizdoš, P.; Dusza, J. Small-Scale Mechanical Testing of Cemented Carbides from the Micro-to the Nano-Level: A Review. *Metals*. **2019**, *9* (5), 502. https://doi.org/10.3390/met9050502

Naughton-Duszová, A.; Halgaš, R.; Bľanda, M.; Hvizdoš, P.; Lofaj, F.; Dusza, J.; Morgiel, J. Nanoindentation of WC–Co Hardmetals. *J. Eur. Ceram. Soc.* **2013**, *33* (12), 2227–2232. https://doi.org/10.1016/J.JEURCERAMSOC.2012.12.018

Nicolás-Morillas, M.; Besharatloo, H.; Alvaredo, P.; Roa, J. J.; Llanes, L.; Gordo, E. Design of alternative binders for hard materials. *Int. J. Refract. Metals Hard Mater.* **2020**, *87*, 105089. https://doi.org/10.1016/j.ijrmhm.2019.105089

Nicolás-Morillas, M.; Llanes, L.; Gordo, E. High-temperature wettability in hard materials: Comparison of systems with different binder/carbide phases and evaluation of C addition. *Int. J. Refract. Metals Hard Mater.* **2023**, *111*, 106081. https://doi.org/10.1016/j.ijrmhm.2022.106081

Nicolás-Morillas, M.; Besharatloo, H.; Cabezas, L.; la Mata, M.; Sales, D. L.; Pereira, L.; Müller-Grunz, A.; Bertalan, C.; Useldinger, R.; Llanes, L.; Gordo, E.; Processing of WC with Fe-based alternative binders: Adjustment of C content and effect of Cr addition. *Int. J. Refract. Metals Hard Mater.* **2024**, *118*, 106444. https://doi.org/10.1016/j.ijrmhm.2023.106444

Olsson, M.; Cinca, N. Mechanisms controlling friction and material transfer in sliding contacts between cemented carbide and aluminum during metal forming. *Int. J. Refract. Metals Hard Mater.* **2024**, *1184*, 106481. https://doi.org/10.1016/j.ijrmhm.2023.106481

Ortiz-Membrado, L.; Cuadrado, N.; Casellas, D.; Roa, J. J.; Llanes, L.; Jiménez-Piqué, E. Measuring the Fracture Toughness of Single WC Grains of Cemented Carbides by Means of Microcantilever Bending and Micropillar Splitting. *Int. J. Refract. Metals Hard Mater.* **2021**, *98*, 105529. https://doi.org/10.1016/j.ijrmhm.2021.105529

Ortner, H. M.; Ettmayer, P.; Kolaska, H. The History of the Technological Progress of Hardmetals. *Int. J. Refract. Metals Hard Mater.* **2014**, *44*, 148–159. https://doi.org/10.1016/j.ijrmhm.2013.07.014

Padmakumar, M. Additive Manufacturing of Tungsten Carbide Hardmetal Parts by Selective Laser Melting (SLM), Selective Laser Sintering (SLS) and Binder Jet 3D Printing (BJ3DP) Techniques. *Lasers in Manufacturing and Materials Processing*. **2020**, *7*, 338–371. https://doi.org/10.1007/s40516-020-00124-0

Perez Delgado, Y.; Bonny, K.; Baets, P.; Neis, P. D.; Rodriguez Fereira, V.; Malek, O.; Vleugels, J.; Lauwers, B. Dry sliding friction and wear response of WC-Co hardmetal pairs in linearly reciprocating and rotating contact. *Sustainable Construction and Design*. **2011**, 12–18.

Pötschke, J.; Berger, C.; Richter, H. J.; Scheithauer, U.; Weingarten, S. Additive manufacturing of hardmetals. In *Proceedings of European Powder Metallurgy*, 2017. https://publica-rest.fraunhofer.de/server/api/core/bitstreams/a474fa1b-4efe-4390-8560-5fd14b276368/content (accessed 2024-01-01).

Prakash, L. *Developments in Tungsten Carbide-Cobalt Cemented Carbides*; Inovar communications, 2008.

Prakash, L. Fundamentals and General Applications of Hardmetals. In *Comprehensive Hard Materials Vol. 1-3*; Sarin, V.; Mari, D.; Llanes, L.; Nebel, C. E., Eds.; Elsevier, 2014; pp 29–90.

Raihanuzzaman, R. M.; Xie, Z.; Hong, S. J.; Ghomashchi, R. Powder Refinement, Consolidation and Mechanical Properties of Cemented Carbides - An Overview. *Powder Technol.* **2014**, *261*, 1–13. https://doi.org/10.1016/j.powtec.2014.04.024

Roa, J. J.; Jimenez-Pique, E.; Verge, C.; Tarragó, J. M.; Mateo, A.; Fair, J.; Llanes, L. Intrinsic Hardness of Constitutive Phases in WC-Co Composites: Nanoindentation Testing, Statistical Analysis, WC Crystal Orientation Effects and Flow Stress for the Constrained Metallic Binder. *J. Eur. Ceram. Soc.* **2015**, *35* (13), 3419–3425. https://doi.org/10.1016/j.jeurceramsoc.2015.04.021

Roa, J. J.; Jiménez-Piqué, E.; Tarragó, J. M.; Sandoval Ravotti, D. A.; Mateo, A.; Fair, J.; Llanes, L. Hall-Petch Strengthening of the Constrained Metallic Binder in WC–Co Cemented Carbides: Experimental Assessment by Means of Massive Nanoindentation and Statistical Analysis. *Materials Science and Engineering: A.* **2016**, *676*, 487–491. https://doi.org/10.1016/J.MSEA.2016.09.020

Roebuck, B.; Almond, E. A. Deformation and Fracture Processes and the Physical Metallurgy of WC–Co Hardmetals. *International Materials Reviews.* **1988**, *33* (2), 90–110. https://doi.org/10.1179/095066088790324094

Roebuck, B.; Klose, P.; Mingard, K. P. Hardness of Hexagonal Tungsten Carbide Crystals as a Function of Orientation. *Acta Mater.* **2012**, *60* (17), 6131–6143. https://doi.org/10.1016/J.ACTAMAT.2012.07.056

Roulon, Z.; Missiaen, J. M.; Lay, S. Carbide Grain Growth in Cemented Carbides Sintered with Alternative Binders. *Int. J. Refract. Metals Hard Mater.* **2020**, *86*, 105088. https://doi.org/10.1016/j.ijrmhm.2019.105088

Sandoval Ravotti, D. A.; Rinaldi, A.; Tarragó, J. M.; Roa, J. J.; Fair, J.; Llanes, L. Scale Effect in Mechanical Characterization of WC-Co Composites. *Int. J. Refract. Metals Hard Mater.* **2018**, *72*, 157–162. https://doi.org/10.1016/J.IJRMHM.2017.12.029

Sandoval Ravotti, D. A. Small-Scale Testing of Micromechanical Response of Cemented Carbides. Thesis (Doctorate), Universitat Politècnica de Catalunya, Barcelona, 2019.

Sandoval Ravotti, D. A.; Roa, J. J.; Ther, O.; Tarrés, E.; Llanes, L. Micromechanical Properties of WC-(W,Ti,Ta,Nb)C-Co Composites. *J. Alloys. Compd.* **2019**, *777*, 593–601. https://doi.org/10.1016/J.JALLCOM.2018.11.001

Sandvik. Understanding cemented carbide. https://pt.scribd.com/document/375993631/SANDVIK-Understanding-cemented-carbide-pdf (accessed 2024-01-01).

Scheithauer, U.; Pötschke, J.; Weingarten, S.; Schwarzer, E.; Vornberger, A.; Moritz, T.; Michaelis, A. Droplet-Based Additive Manufacturing of Hard Metal Components by Thermoplastics 3D Printing. *J. Ceram. Sci. Tech*. **2017**, *8* (1), 155–160. https://doi.org/10.4416/JCST2016-00104

Shatov, A. V.; Ponomarev, S. S.; Firstov, S. A. Hardness and Deformation of Hardmetals at Room Temperature. In *Comprehensive Hard Materials Vol. 1-3*; Sarin, V.; Mari, D.; Llanes, L.; Nebel, C. E., Eds.; Elsevier, 2014a; pp 267–299. https://doi.org/10.1016/B978-0-08-096527-7.00009-X

Shatov, A. V.; Ponomarev, S. S.; Firstov, S. A. Fracture and strength of hardmetals at room temperature. In *Comprehensive Hard Materials Vol. 1-3*; Sarin, V.; Mari, D.; Llanes, L.; Nebel, C. E., Eds.; Elsevier, 2014b; pp 301–343. https://doi.org/10.1016/B978-0-08-096527-7.00010-6

Sheikh, S.; M'Saoubi, R.; Flasar, P.; Schwind, M.; Persson, T.; Yang, J.; Llanes, L. Fracture toughness of cemented carbides: Testing method and microstructural effects. *Int. J. Refract. Metals Hard Mater.* **2015**, *49*, 153–160. https://doi.org/10.1016/j.ijrmhm.2014.08.018

Sribalaji, M.; Mukherjee, B.; Islam, A.; Kumar Keshri, A. Microstructural and Mechanical Behavior of Spark Plasma Sintered Titanium Carbide with Hybrid Reinforcement of Tungsten Carbide and Carbon Nanotubes. *Materials Science and Engineering: A.* **2017**, *702*, 10–21. https://doi.org/10.1016/j.msea.2017.06.108

Steinlechner, R.; Oro Calderon, R.; Koch, T.; Linhardt, P.; Schubert, W. D. A Study on WC-Ni Cemented Carbides: Constitution, Alloy Compositions and Properties, Including Corrosion Behaviour. *Int. J. Refract. Metals Hard Mater.* **2022**, *103*, 105750. https://doi.org/10.1016/j.ijrmhm.2021.105750

Straumal, B.; Konyashin, I. WC-Based Cemented Carbides with High Entropy Alloyed Binders: A Review. *Metals* **2023**, *13*, 171. https://doi.org/10.3390/met13010171

Suzuki, A.; Inui, H.; Pollock, T. M. L12-Strengthened Cobalt-Base Superalloys. *Annu. Rev. Mater. Res.* **2015**, *45*, 345–368. https://doi.org/10.1146/ANNUREV-MATSCI-070214-021043

Tang, W.; Zhang, L.; Zhu, J. fei; Chen, Y.; Tian, W.; Liu, T. Effect of Direct Current Patterns on Densification and Mechanical Properties of Binderless Tungsten Carbides Fabricated by the Spark Plasma Sintering System. *Int. J. Refract. Metals Hard Mater.* **2017**, *64*, 90–97. https://doi.org/10.1016/j.ijrmhm.2017.01.010

Tang, T.; Xiao, X.; Xu, K.; Lou, M.; Hu, X.; Li, S.; Zhang, W.; Fan, Z.; Chang, K. Corrosion-Resistant WC-Co Based Cemented Carbides: Computational Design and Experimental Verification. *Int. J. Refract. Metals Hard Mater.* **2023**, *110*, 106044. https://doi.org/10.1016/J.IJRMHM.2022.106044

Tarragó, J. M.; Jiménez-Piqué, E.; Schneider, L.; Casellas, D.; Torres, Y.; Llanes, L. FIB/FESEM Experimental and Analytical Assessment of R-Curve Behavior of WC-Co Cemented Carbides. *Materials Science and Engineering: A.* **2015**, *645*, 142–149. https://doi.org/10.1016/j.msea.2015.07.090

Trueba, M.; Aramburu, A.; Rodríguez, N.; Iparraguirre, I.; Elizalde, M. R.; Ocaña, I.; Sánchez, J. M.; Martínez-Esnaola, J. M. "In-Situ" Mechanical Characterisation of WC–Co Hardmetals Using Microbeam Testing. *Int. J. Refract. Metals Hard Mater.* **2014**, *43*, 236–240. https://doi.org/10.1016/J.IJRMHM.2013.12.005

Upadhyaya, G. S. *Nature and Properties of Refractory Carbides*; Nova Science Publishers, 1996.

Upadhyaya, G. S. *Cemented Tungsten Carbides: Production, Properties and Testing*; Noyes Publications, 1998.

Upadhyaya, G. S. Materials Science of Cemented Carbides—an Overview. *Mater. Des.* **2001**, *22* (6), 483–489.

Wachowicz, J.; Kruzel, R.; Bałaga, Z.; Ostrowska, A.; Dembiczak, T. Application of U-FAST Technology in Sintering of Submicron WC-Co Carbides. *Materials.* **2023**, *16* (6), 2450.

Walbrühl, M.; Linder, D.; Ågren, J.; Borgenstam, A. Alternative Ni-Based Cemented Carbide Binder – Hardness Characterization by Nano-Indentation and Focused Ion Beam. *Int. J. Refract. Metals Hard Mater.* **2018**, *73*, 204–209. https://doi.org/10.1016/j.ijrmhm.2018.02.017

Wang, J.; Zuo, D.; Zhu, L.; Li, W.; Tu, Z.; Dai, S. Effects and Influence of Y2O3 Addition on the Microstructure and Mechanical Properties of Binderless Tungsten Carbide Fabricated by Spark Plasma Sintering. *Int. J. Refract. Metals Hard Mater.* **2018**, *71*, 167–174. https://doi.org/10.1016/j.ijrmhm.2017.11.016

Warren, R. Solid-Liquid Interfacial Energies in Binary and Pseudo-Binary Systems. *J. Mater. Sci.* **1980**, *15* (10), 2489–2496. https://doi.org/10.1007/BF00550752/METRICS

Wolfe, T. A.; Shah, R. M.; Prough, K. C.; Trasorras, J. L. Binder Jetting 3D Printed Cemented Carbide: Mechanical and Wear Properties of Medium and Coarse Grades. *Int. J. Refract. Metals Hard Mater.* **2023a**, *113*. https://doi.org/10.1016/j.ijrmhm.2023.106197

Wolfe, T.; Shah, R.; Prough, K.; Trasorras, J. L. Coarse Cemented Carbide Produced via Binder Jetting 3D Printing. *Int. J. Refract. Metals Hard Mater.* **2023b**, *110*, 106016. https://doi.org/10.1016/j.ijrmhm.2022.106016

Xu, Z. H.; Ågren, J. A Modified Hardness Model for WC–Co Cemented Carbides. *Materials Science and Engineering: A.* **2004**, *386*(1–2), 262–268. https://doi.org/10.1016/J.MSEA.2004.07.061

Xu, H.; Huang, H. Microstructure Evolution and Mechanical Properties of Thermally Sprayed Coating Modified by Laser Remelting and Injection with Tungsten Carbide. *Ceram. Int.* **2022a**, *48* (16), 22854–22868. https://doi.org/10.1016/j.ceramint.2022.04.189

Xu, H.; Huang, H. Plasma Remelting and Injection Method for Fabricating Metal Matrix Composite Coatings Reinforced with Tungsten Carbide. *Ceram. Int.* **2022b**, *48* (2), 2645–2659. https://doi.org/10.1016/j.ceramint.2021.10.048

Yang, Y.; Zhang, C.; Wang, D.; Nie, L.; Wellmann, D.; Tian, Y. Additive Manufacturing of WC-Co Hardmetals: A Review. *Int. J. Adv. Manuf. Tech.* **2020**, *108* (5–6), 1653–1673. https://doi.org/10.1007/s00170-020-05389-5

Zak Fang, Z.; Koopman. M. C. Cemented Tungsten Carbide Hardmetal-An Introduction. In *Comprehensive Hard Materials*; Sarin, V. K., Mari, D., Llanes, L., Nebel, C. E., Eds.; Elsevier, 2014; pp 123-137. https://doi.org/10.1016/B978-0-08-096527-7.00004-0

Zhao, Z.; Liu, F.; Zhao, M.; Zhong, L.; Xu, Y.; Li, J. A New Strategy to Efficiently Fabricate Tungsten Carbide Coating on Tungsten: Two-Step Interstitial Carburization. *Surf. Coat. Technol.* **2020**, *389*, 125579. https://doi.org/10.1016/j.surfcoat.2020.125579

Zheng, Y. F.; Fargas, G.; Besharatloo, H.; Serra, M.; Roa, J. J.; Armelin, E.; Lavigne, O.; Llanes, L.; Assessment of corrosion-induced changes on the mechanical integrity of cemented carbides at small length scales. *Int. J. Refract. Metals Hard Mater.* **2019**, *84*, 105033, https://doi.org/10.1016/j.ijrmhm.2019.105033

Zheng, Y.F.; Fargas, G.; Lavigne, O.; Serra, M.; Coureaux, D.; Zhang, P.P.; Yao, Z.H.; Zhang, Q.L.; Yao, J.H.; Llanes, L. Contact fatigue of WC-6%wtCo cemented carbides: Influence of corrosion-induced changes on emergence and evolution of damage, *Ceram. Int.* **2022a**, *48*, 5766-5774. https://doi.org/10.1016/j.ceramint.2021.11.124

Zheng, Y.; Fargas, G.; Armelin, E.; Lavigne, O.; Zhang, Q.; Yao, J.; Llanes, L. Influence of Corrosion-Induced Damage on Mechanical Integrity and Load-Bearing Capability of Cemented Carbides. *Metals.* **2022b**, *12*, 2104. https://doi.org/10.3390/met12122104

Zhou, P. F.; Xiao, D. H.; Yuan, T. C. Comparison between Ultrafine-Grained WC–Co and WC–HEA-Cemented Carbides. *Powder Metallurgy.* **2016**, *60* (1), 1–6. https://doi.org/10.1080/00325899.2016.1260903

Zhou, P. L.; Xiao, D. H.; Zhou, P. F.; Yuan, T. C. Microstructure and Properties of Ultrafine Grained AlCrFeCoNi/WC Cemented Carbides. *Ceram. Int.* **2018**, *44* (14), 17160–17166. https://doi.org/10.1016/J.CERAMINT.2018.06.171